Cancer Research

M2 Macrophage-Derived Exosomes Promote Cell Migration and Invasion in Colon Cancer

Jingqin Lan[1], Li Sun[2], Feng Xu[1], Lu Liu[1], Fuqing Hu[1], Da Song[1], Zhenlin Hou[1], Wei Wu[1], Xuelai Luo[1], Jing Wang[3], Xianglin Yuan[2], Junbo Hu[1], and Guihua Wang[1]

Abstract

Clinical and experimental evidence has shown that tumor-associated macrophages promote cancer initiation and progression. However, the macrophage-derived molecular determinants that regulate colorectal cancer metastasis have not been fully characterized. Here, we demonstrate that M2 macrophage–regulated colorectal cancer cells' migration and invasion is dependent upon M2 macrophage–derived exosomes (MDE). MDE displayed a high expression level of miR-21-5p and miR-155-5p, and MDE-mediated colorectal cancer cells' migration and invasion depended on these two miRNAs. Mechanistically, miR-21-5p and miR-155-5p were transferred to colorectal cancer cells by MDE and bound to the BRG1 coding sequence, downregulating expression of BRG1, which has been identified as a key factor promoting the colorectal cancer metastasis, yet is downregulated in metastatic colorectal cancer cells. Collectively, these findings show that M2 macrophages induce colorectal cancer cells' migration and invasion and provide significant plasticity of BRG1 expression in response to tumor microenvironments during malignant progression. This dynamic and reciprocal cross-talk between colorectal cancer cells and M2 macrophages provides a new opportunity for the treatment of metastatic colorectal cancer.

Significance: These findings report a functional role for miRNA-containing exosomes derived from M2 macrophages in regulating migration and invasion of colorectal cancer cells.

Introduction

Tumor-associated macrophages (TAM) are the major player and orchestrate various factors in tumor microenvironment to facilitate tumor progression (1–4). In general, macrophages can be polarized to M1 or M2 macrophages. M1-polarized macrophages are activated by cytokines such as IFNγ and produce proinflammatory and immunostimulatory cytokines (IL12, TNFα etc.; ref. 5). However, TAMs are thought to more closely resemble M2-polarized macrophages, which are activated by Th2 cytokines (IL4, IL10, and IL13; refs. 6, 7). It has been reported that TAMs can promote proliferation, invasion, and metastasis of tumor cells, stimulate tumor-related angiogenesis, and inhibit antitumor immune response, following with the progression of tumor (8–11). With the unraveling of the relationship between TAMs and tumors, TAMs are now being recognized as potential therapeutic targets for cancer. However, the mechanisms of TAMs promoting cancer metastasis and the communication between TAMs and tumor cells are still waiting for exposure.

In recent years, the function of exosomes has evoked increased interest in cancers. Exosomes are lipid bilayer membrane vesicles (50–100 nm) derived from the luminal membrane of multivesicular bodies, which are constitutively released by fusion with the cell membrane (12–17). Exosomes have been explored as the key factor in mediating tumor cell and microenvironment cell communication. In turn, they play important roles in the promotion of tumor growth, tumorigenesis, tumor angiogenesis, tumor immune escape, drug resistance, and metastasis (18–20). In particular, exosomes have been served as promising biomarkers for cancer diagnosis and even as potential treatment targets for patients with cancer.

In this study, we find that the M2 macrophages take responsibility for colon cancer cell migration and invasion by macrophage–derived exosomes (MDE). We demonstrate that a remarkable downregulation of BRG1 is in response to MDE, which contain miR-21-5p and miR-155-5p, the miRNAs targeting BRG1. Our findings unveil a new sight between tumor cells and the TAMs: specific miRNAs are directly shuttled from M2 macrophages via exosomes to colorectal cancer cells, targeting and downregulating BRG1 expression, in turn promoting colorectal cancer cells' migration and invasion.

Materials and Methods

Cell lines and cell culture

All colorectal cancer cell lines (SW48, SW480, and CO-115) and human umbilical vein endothelial cells (HUVEC) were purchased from ATCC. Cell authentication and *Mycoplasma* testing were conducted, using RT-PCR detection for *Mycoplasma* and 10 short

[1]GI Cancer Research Institute, Tongji Hospital, Huazhong University of Science and Technology, Wuhan, China. [2]Department of Oncology, Tongji Hospital, Huazhong University of Science and Technology, Wuhan, China. [3]Department of Immunology, Basic of Medicine, Tongji Medical College, Huazhong University of Science and Technology, Wuhan, China.

Note: Supplementary data for this article are available at Cancer Research Online (http://cancerres.aacrjournals.org/).

J. Lan and L. Sun contributed equally to this article.

Corresponding Authors: Guihua Wang, Tongji Hospital, Tongji Medical College, Wuhan, Hubei 430030, China. Phone: 8627-8366-5275; Fax: 8627-8366-2696; E-mail: ghwang@tjh.tjmu.edu.cn; and Junbo Hu, Tongji Hospital, Tongji Medical College, Wuhan, Hubei 430030, China. Phone: 8627-8366-5275; Fax: 8627-8366-2696; E-mail jbhu@tjh.tjmu.edu.cn

doi: 10.1158/0008-5472.CAN-18-0014

tandem repeat identifications by capillary electrophoresis for cell line authentication. cancer-associated fibroblasts (CAF) were derived from patients and validated by immunofluorescence. All cell lines were cultured in recommended medium supplemented with 10% FBS and were used for experiments within 50 passaging culture. M2 macrophages were isolated as protocol described by Jeffrey W. Pollard (21). Considering the complex ingredients of FBS, all of conditioned medium (CM) was collected after the cells were cultured in serum-free DMEM for 12 hours and filtered through a 0.22-μm filter (Merck Millipore) to remove cells and cellular debris.

TAMs were isolated from colorectal cancer tissues (refer to Tumor Microenvironment Study Protocols by Springer). Fresh specimens were cut into small pieces and digested at 37°C for 45 minutes under continuous rotation. After removing the red blood cells, cells were labeled with CD68 and CD163 antibodies. $CD68^+/CD163^+$ cells were purified using magnetic cell separation or FACS.

Isolation of exosomes and purification

Exosomes were collected from M2 macrophage medium after ultracentrifugation as described previously (22). Briefly, conditioned medium was centrifuged at 500 × *g* for 15 minutes, at 3,000 × *g* for 15 minutes, and at 12,000 × *g* for 30 minutes at 4°C to remove cells and debris. The exosomes were purified by centrifugation at 140,000 × *g* for 80 minutes. After resuspension in PBS, they were repeatedly purified by ultracentrifugation as the last step. Exosomes were resuspended with (i) 2% glutaraldehyde in 0.1 mol/L phosphate buffer for transmission electron microscopy (22); (ii) RIPA buffer for Western blot analysis or precooled exosome resuspension buffer for total exosome RNA isolation; and (iii) FBS-free medium for cell treated and tested *in vivo*.

Luciferase activity assay

Luciferase reporter assays were done as described previously in manufacturer's protocol. The wild-type BRG1-3′untranslated regions (UTR) or the BRG1-3′UTRs with various miRNA-binding site mutations driven by psiCHECK-2 luciferase reporter were transfected into tumor cells using Lipofectamine 3000 (Life Technologies). After 48 hours, tumor cells were cocultured with isolated exosomes. Another 24 hours later, luciferase activities were measured by Dual-Luciferase Report Assay Kit (Promega) on Turner BioSystems Instrument.

Western blotting

Western blotting was done as described previously. Cells or exosomes were collected and denatured. Proteins were separated by SDS-PAGE gel and transferred onto polyvinylidene difluoride membranes. After blocked in 5% skim milk for 30 minutes, membranes were probed with various primary antibodies overnight at 4°C, followed by incubation with horseradish peroxidase–linked secondary antibodies for 1 hour at room temperature, and visualized with electrochemiluminescence by the chemiluminescence instrument.

Cell motility and migration assays

The effect of exosomes on the migration and invasion of cancer cells was determined by using transwell 24-well plates (8-μm pores; Corning). Cells across pores were fixed with 4% paraformaldehyde and stained with 1% crystal violet solution. For each chamber, three fields were randomly chosen and cells were counted.

IHC

IHC images were analyzed as follows: after CD163 detection by primary antibody on human colorectal cancer samples, three fields were chosen from each slide by two experienced pathologists on three high-power (×100) microscopic fields (HPF) in "hotspots" (areas with high cellular density).

BRG1 staining intensity was categorized: no staining as 0, weak as 1, moderate as 2, and strong as 3. The percentage of cells stained was categorized: no positive cells as 0, less than 25% positive cells as 1, 25%–50% positive cells as 2, 50%–75% positive cells as 3, and more than 75% positive cells as 4. We calculated the score of each sample by multiplying the BRG1 staining intensity with the percentage scale. The results suggested that M2–CM and M2–exosomes could reduce BRG1 expression.

Antibodies

Anti-CD206 antibodies were purchased from BD Biosciences (BD 551135, 20 μL for immunofluorescence and flow cytometry per test). Anti-GAPDH (sc-47724, 1:1,000 for Western blot analysis), anti-BRG1(sc-17796, 1:500 for Western blot analysis, 1:50 for IHC), anti-CD81 (sc-7637, 1:500 for Western blot analysis), and anti-CD63 (sc-5275, 1:500 for Western blot analysis). Anti-CD68 antibodies were purchased from Abcam (ab49777, 1:40 dilution for IHC). Anti-CD68 (12-0689) and anti-163 (12-1639) antibodies were purchased from eBioscience (5 μL per test). Anti-calnexin antibodies were purchased from Cell Signaling Technology (2679, 1:1,000 for Western blot analysis).

Transmission electron microscopy

Isolated exosomes were mixed with 4% paraformaldehyde. Exosomes were then dropped onto Formvar carbon–coated electron microscopy grids and fixed with 1% glutaraldehyde for 10 minutes. Samples were negatively stained with 2% uranyl acetate solution. Images were obtained using a Tecnai transmission electron microscope at 163 kV.

In vivo experiments

The Institutional Animal Care and Use Committee of Huazhong University of Science and Technology has approved our animal studies. All animal experiments were carried out in accordance with the Animal Study Guidelines of Huazhong University of Science and Technology. Four-to-5 weeks old female BALB/c nude mice were used. Five female nude mice were inoculated per group. A total of 5×10^5 SW48 cells, SW48 cells with CM, or SW48 cells with exosomes were coinjected into the caudal veins using ultra-fine insulin syringe by BD Biosciences. CM or exosomes (10 μg) were then injected into caudal veins every 3 days after exosomes were stained with DiI. Animals were sacrificed 6 weeks postinjection. The number of metastatic lungs, number of clones in lungs, and small metastatic foci were compared in the three groups. DiI was purchased from Sigma-Aldrich.

To observe the mice survival curves, the experiments *in vivo* would be repeated. But the mice would be kept for 2 months and the death time of each mouse was recorded.

RNA sequencing using Illumina HiSeq 2500

Exosomes were isolated from TAM cultures. Total RNAs in exosomes were extracted using the Total Exosome RNA and Protein Isolation Kit (Invitrogen by Life Technologies). SW48-exo were SW48 cells cocultured with TAM-derived exosomes for 24 hours. SW48 FBS–free were cultured in FBS-free medium,

which were used for resuspending exosomes. Total RNAs of cells were extracted using traditional protocols. The amount and quality of small RNA in the total RNA were tested by Ribobio Co. Ltd. Small RNA library construction and sequencing was performed by Ribobio Co. Ltd. Then the cDNA library was sequenced on Illumina Hiseq 2500. Raw reads were collected using related Illumina analysis software.

miRNA, RNAi, and construction of adenoviral systems

Synthetic miRNAs, miRNA inhibitors, and Cy3-labeling miRNAs were synthesized and purified by RiBo (RiboBio Co.). RNA oligonucleotides were transfected by using Lipofectamine 2000 (Invitrogen) and the medium was replaced 6 hours after transfection. Cy3-labeled miRNAs were transfected into macrophages with using Lipofectamine 3000 (Invitrogen). Macrophages containing Cy3 miRNA were cocultured with SW48 cells and samples were examined using fluorescence microscope and flow cytometry.

DiI-labeled exosomes transfer assay

Purified exosomes isolated from $CD163^+$ macrophages were suspended in 1,000 μL and incubated with 10 μL DiI for 30 minutes at 37°C.

Patient samples

Our study was conducted in accordance with U.S. Common Rule, and archived primary colorectal cancer paraffin-embedded specimens ($n = 61$) were collected under a Human Research Ethics Committees protocol at Tongji Hospital (Wuhan, China) with patients' written formal consent. These patients have been followed over time.

Statistical analysis

GraphPad Prism 5.0 software was used to conduct statistical analyses. Kaplan–Meier analysis was used to calculate the survival differences between divided groups. The Pearson r correlation was taken for correlation analysis of mRNA expression from The Cancer Genome Atlas (TCGA). Two groups of data were analyzed by two-tailed *t* tests.

Results

MDE enhances colorectal cancer cell mobility, migration, and invasion

M2 macrophages were obtained from clinical colon cancer specimens and cultured as mentioned in the Materials and Methods section. Cells were positive for M2 macrophage markers such as CD68, CD163, and CD206, which was confirmed by immunostaining (Fig. 1A; Supplementary Fig. S1A). CM was harvested from M2 macrophages. Scratch test was employed to examine the effects of M2 macrophages CM on cell mobility in SW48 colon cancer cells (Fig. 1B). Compared with control cells, CM of M2 macrophages–treated SW48 cells showed increased mobility. Then, Boyden chamber assay was performed and SW48 cells treated by CM of M2 macrophages explored an increased number in cell migration compared with the corresponding cells treated by FBS-free medium (Fig. 1C, left). In addition, we soaked Matrigel onto modified Boyden chambers first and then performed Transwell assay. SW48 cells treated with CM showed higher ability in cell invasion (Fig. 1C, right).

Recently studies have demonstrated that exosomes are released by a variety of cells involved in cancer metastasis (23). In turn, we hypothesized that exosomes might actively mediate tumor metastasis in our experimental system. We isolated exosomes from M2 macrophages in a manner of ultracentrifugation or total exosome isolation reagent. These exosomes were tested by particle size analyzer, which reveals a diameter of 100 nm (Supplementary Fig. S1B). Isolated exosomes appeared as rounded particles with approximately 80–100 nm size and a double-layer membrane (Fig. 1D). CD63 and CD81 are surface antigens commonly used as exosomal markers. Our isolated exosomes were confirmed using Western blot analysis with the exosome-specific markers, CD81 and CD63 (Supplementary Fig. S1C). Calnexin is an integral protein of the endoplasmic reticulum, which is used here for negative control. Next, we detected whether these exosomes could be internalized by colorectal cancer cells. Exosomes were labeled with DiI, a lipophilic fluorescentcarbocyamine dye. We added the same concentration of DiI into FBS-free medium and this medium was treated as same as the DiI- labeled exosomes. These media were added into the SW48 cells as control group. Fluorescence microscope and flow cytometer was used to confirm that colorectal cancer cells could uptake exosomes derived from $CD163^+$ macrophage (Fig. 1E; Supplementary Fig. S1D). We assumed that MDE may promote colon cancer metastasis. Scratch test showed that exosomes derived from M2 macrophage (M2-exo)-treated SW48 cells showed increased mobility (Fig. 1F). We performed migration and invasion assays using groups including (i) medium-depleted FBS, (ii) full M2 macrophage–derived CM, (iii) M2 macrophage–derived exosomes alone, and (iv) M2 macrophages–derived CM depletion of exosomes. Interestingly, we got a similar result that exosomes derived from M2 macrophages could promote colon cancer cells' mobility, migration, and invasion (Fig. 1G). The effects of exosomes derived from M2 macrophages were also detected with SW480 cell line (Supplementary Fig. S2A–S2D). Collectively, our data indicated that M2 macrophages mediated positively and colorectal cancer metastasis is partially dependent on MDE.

Exosomes isolated from $CD163^+$ macrophages promote colon cancer cell invasion and migration *in vivo*

To determine whether exosomes isolated from M2 macrophages prime colon cancer metastasis, we treated $SW48^{Luc}$ with M2-CM, M2-exo, and FBS-free medium. Then, these three groups were injected into caudal veins of female nude mice and we injected CM, DiI-labeled exosomes, and FBS-free medium into corresponding mice every 3 days. As shown in Fig. 2A, significantly larger tumors were formed by cells treated by CM and M2 exosomes. The survival curve of mice in each group showed that all of the CM or exosome-treated mice died 55 days after injection, whereas 40% of the FBS-free media–treated mice remained alive (Fig. 2B) and CM and exosomes initiated more migration in lungs (Fig. 2C). Histologic analysis showed that CM and exosomes significantly increased the migration nodules, and CM exhibited more severe results than exosomes (Fig. 2D). Moreover, we also use immunofluorescence staining to show that red-labeling exosomes were detected in some of the cancer cells (Fig. 2E). These results suggested that exosomes could be transferred to cancer cells and promote cancer invasion and migration *in vivo*.

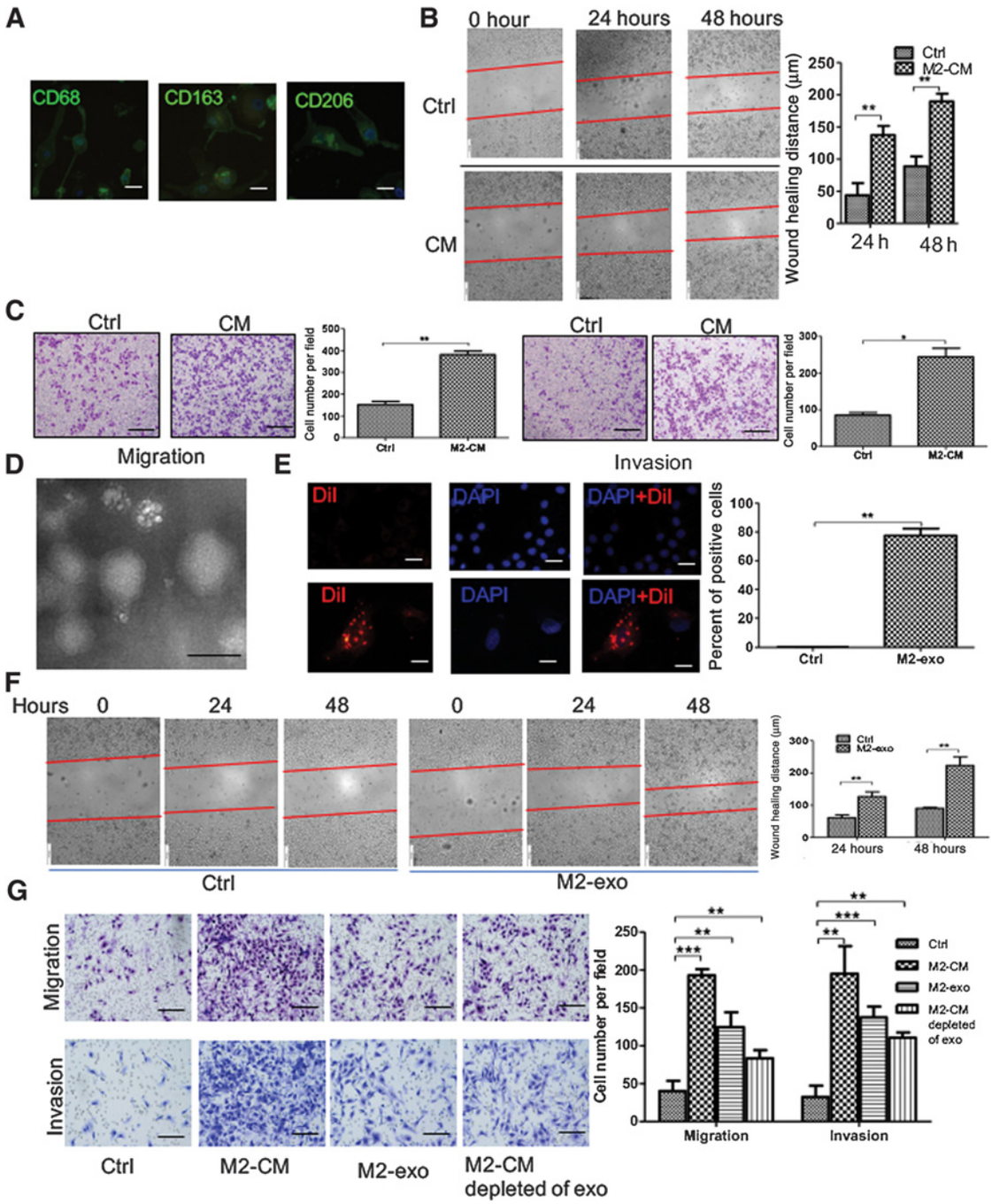

Figure 1.

M2-derived exosomes enhance colorectal cancer cell mobility, migration, and invasion. **A,** M2 macrophages were validated by positive immunostaining for M2 macrophages markers. Scale bar, 2 μm. **B,** Wound-healing assay. SW48 cells were treated with M2-CM and cell monolayers were scratched 1–200 μL yellow tips. Images were taken 0, 24, and 48 hours after wounding scratch (left, representative pictures; right, the quantitative migrating distance). Scale bar, 200 μm. The red lines mark the original wound, whereas the cells moved the wound closer. The *y*-axis of the graph is the distance the cells moved. **C,** Cell migration assays and invasion assays using Transwell or Matrigel-coated Transwell in SW48 treated without or with M2-CM (left, representative pictures of Transwell chambers; scale bar, 200 μm; right, average counts from three times of independent test; **, $P < 0.01$; *, $P < 0.05$). **D,** Transmission electron microscopic image of the M2 exosomes. Scale bar, 100 nm. **E,** Exosomes derived from M2 macrophage were added to SW48 cells. Left, a fluorescent microscope was used to detect red signals in SW48 cells. Scale bar, 2 μm. Right, flow cytometry detected the DiI in SW48 cells. **F,** Wound-healing assay. SW48 cells were treated with M2 exosomes and cell monolayers were scratched 1–200 μL yellow tips. Images were taken 0, 24, and 48 hours after wounding scratch (left, representative pictures; right, the quantitative migrating distance). **, $P < 0.01$. **G,** Cell migration assays and invasion assays using Transwell or Matrigel-coated Transwell. Scale bar, 200 μm. **, $P < 0.01$; ***, $P < 0.001$.

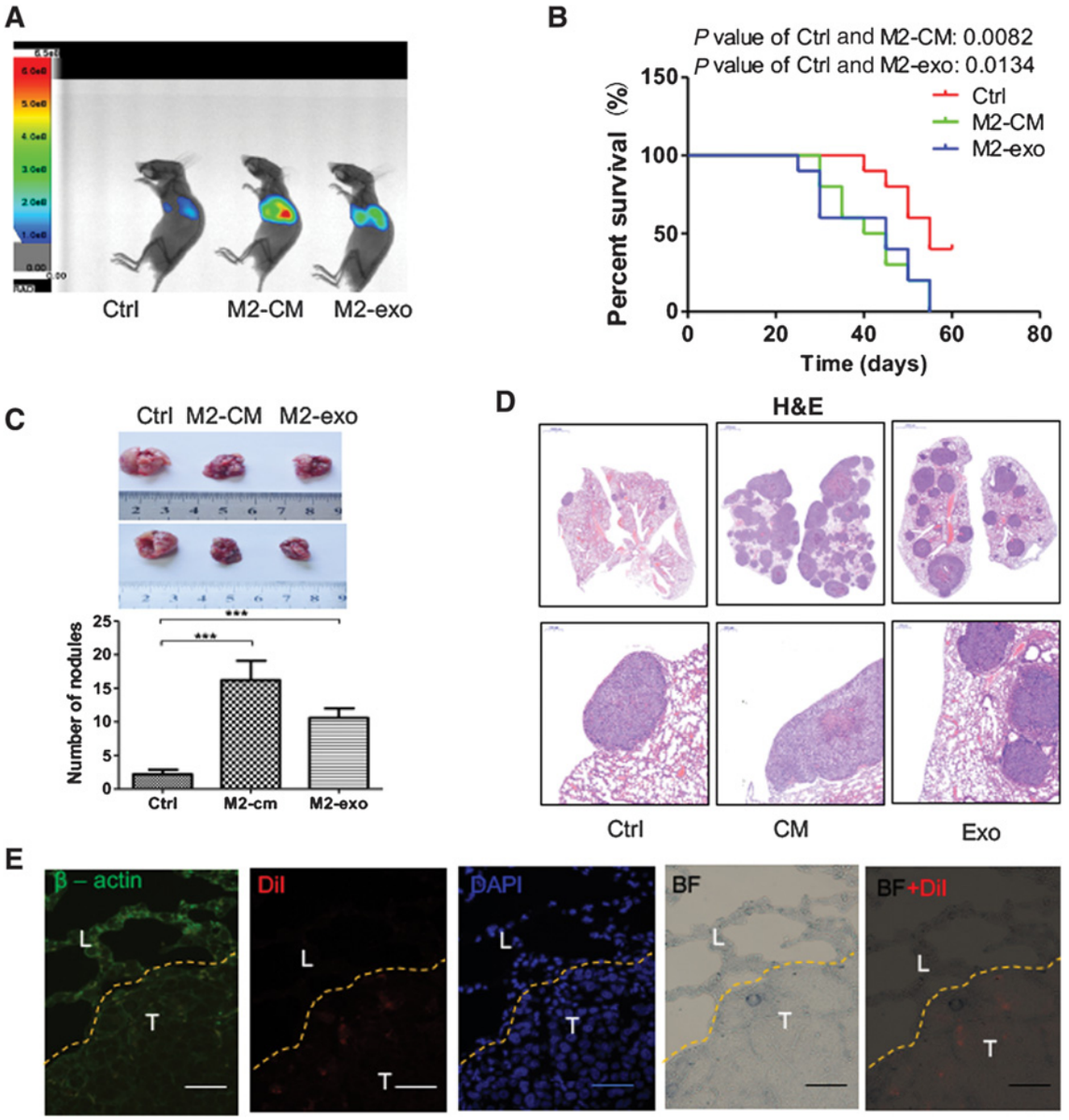

Figure 2.

Exosomes isolated from CD163^{+} macrophages promote colon cancer cell invasion and migration *in vivo*. SW48^{Luc} cells were cocultured with M2-CM or M2-exo, collected, and injected into caudal veins of female nude mice (5 mice for each group). CM, DiI-labeled exosomes, and FBS-free medium were injected into corresponding mice every 3 days. **A,** Bioluminescence imaging was performed in 3 weeks. **B,** The mice survival curves of each group during 60 days. Control (Ctrl) mice and M2-CM mice, $P < 0.01$; control mice and M2-exo mice, $P < 0.05$. **C,** All of the mice were sacrificed and the lungs were collected. Top, visible lung metastases are shown. Bottom, quantitative average number of visible lung metastases analysis in control mice, M2-CM mice, and M2-exo mice. **D,** Hematoxylin and eosin (H&E) staining in SW48 cells' lung metastatic site. Top scale bar, 2,000 μm; bottom scale bar, 200 μm. **E,** Fluorescent microscope was used to detect red signals (DiI-stained exosomes) in lung metastases. Scale bar, 50 μm.

MDE regulates colorectal cancer cells' migration and invasion depending on miRNAs

It has been reported that exosomes are highly heterogeneous and likely reflect the phenotypic state of the cell that generates them (24). Just like cells, exosomes are composed of a lipid bilayer and can contain all known molecular constituents of a cell, including proteins, RNA, and DNA (25). To identify the mechanisms that MDE-promoted colorectal cancer cells' migration and invasion, we performed an RNAsequencing screening using the RNA from MDE (Supplementary Fig. S3A). We compared the miRNA profiles of SW48 cells, M2 macrophages exosomes and SW48 treated by M2 macrophages exosomes (Supplementary Fig. S3B; Supplementary Table S1). As shown in Supplementary Fig. 3B, noncoding RNA sequence analysis revealed three miRNAs that had altered expression between SW48 and SW48 treated with M2-derived exosomes: miR-155-5p,

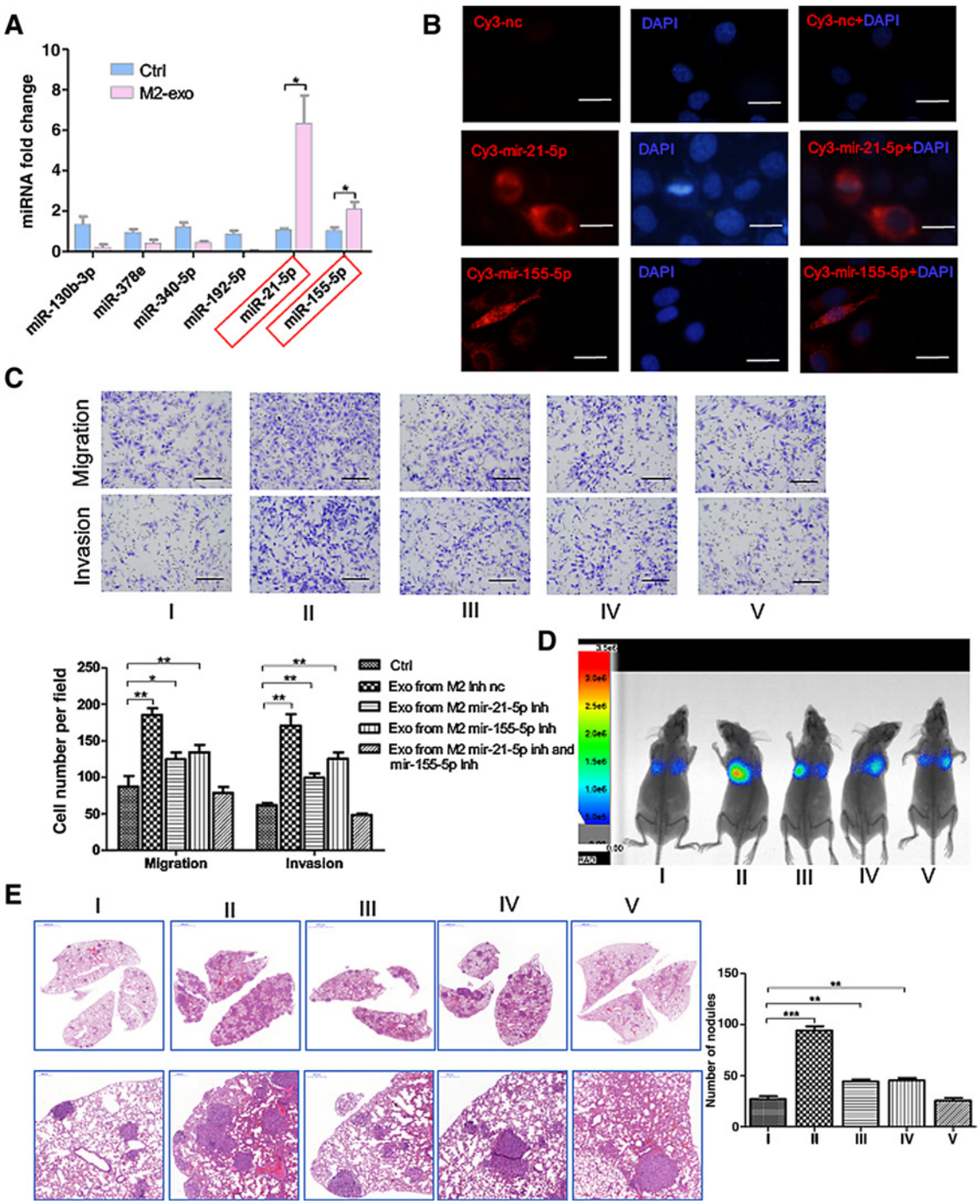

Figure 3.

MDE transport miR-21-5p and miR-155-5p into colon cancer cells. **A,** qRT-PCR analysis of miRNA expression in SW48 incubated without or with M2-exo. *, $P < 0.05$. **B,** Images were taken 48 hours after SW48 cells were cocultured with M2 transfected with Cy3-labeled miR-21-5p or miR-155-5p. Scale bar, 2 μm. **C,** Cell migration and invasion assays using Transwell or Matrigel-coated Transwell in SW48 treated with (i) FBS-free medium, (ii) exosomes from M2 transfected with inhibitor negative control, (iii) exosomes from M2 transfected with miR-21-5p inhibitor, (iv) exosomes from M2 transfected with miR-155-5p inhibitor, and (v) exosomes from M2 transfected with miR-155-5p inhibitor (top representative images, average counts from three random microscopic fields; *, $P < 0.05$; **, $P < 0.01$). **D** and **E,** SW48^{Luc} cells were cocultured with (i) FBS-free medium, (ii) exosomes from M2 transfected with inhibitor negative control, (iii) exosomes from M2 transfected with miR-21-5p inhibitor, (iv) exosomes from M2 transfected with miR-155-5p inhibitor, and (v) exosomes from M2 transfected with miR-155-5p inhibitor. miR-155-5p, exosomes, and FBS-free medium were injected into corresponding mice every 3 days. Bioluminescence imaging was performed in 3 weeks (**D**) and hematoxylin and eosin staining in SW48 cells lung metastatic site (top left, 2,000 μm; bottom left, 200 μm; right, quantitative average number of visible lung metastases analysis; **E**).

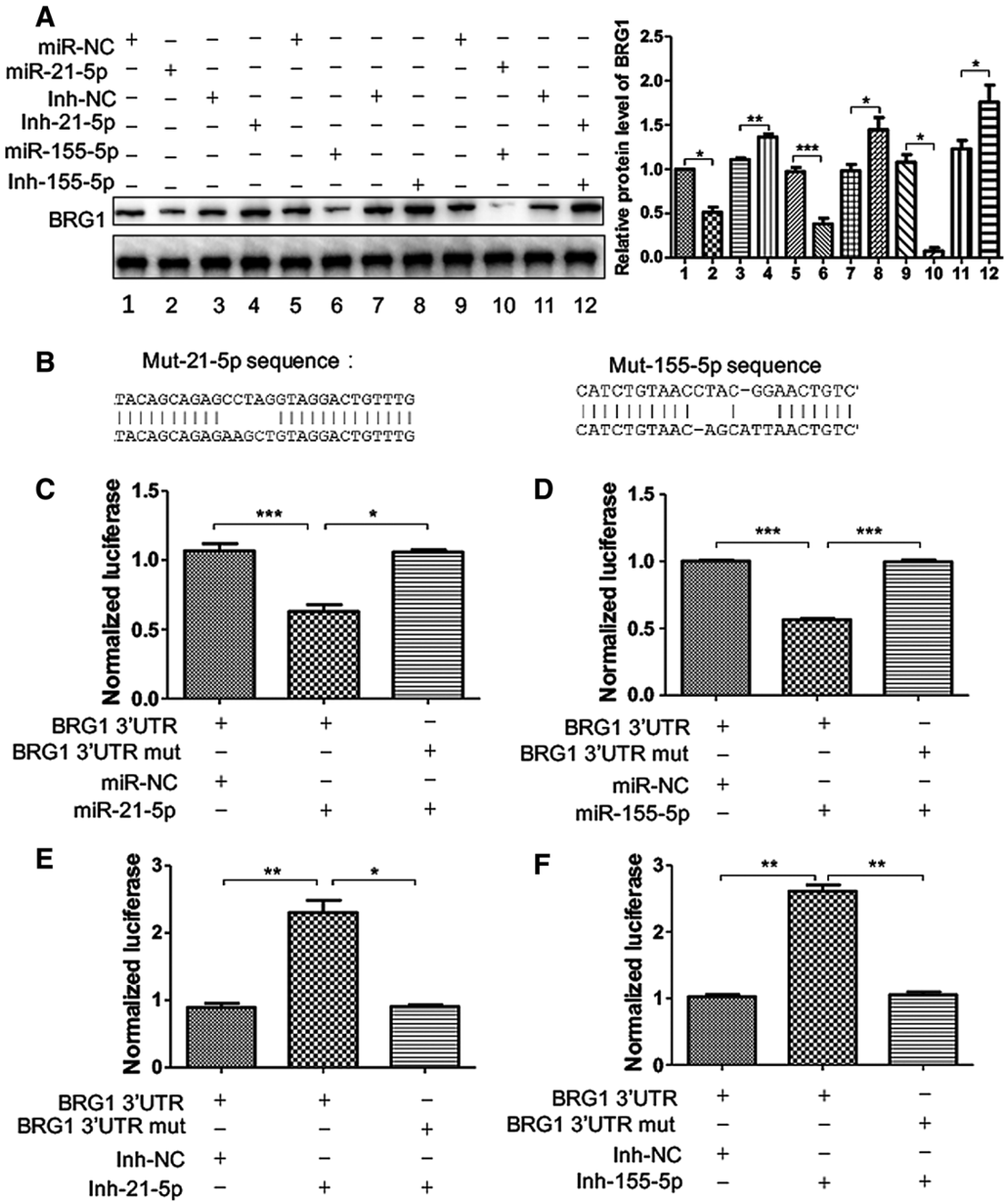

Figure 4.

BRG1 is the target of miR-21-5p and miR-155-5p. **A,** The protein expression analysis of BRG1 in SW48 cells 72 hours after transfection with miR-21-5p mimics (miR-21-5p), miR-155-5p mimics (miR-155-5p), or the negative control (miR-NC) and miR-21-5p inhibitor (Inh-21-5p), miR-155-5p inhibitor (Inh-155-5p), or the negative control (Inh-NC; right, the relative protein level of BRG1 based on three independent tests). **B,** Schematic representation of the 3′-UTR of BRG1 with the predicted target site for miR-21-5p and miR-155-5p. The mutant site of BRG1 3′-UTR is indicated (without line). **C,** Reporter constructs containing either wild-type BRG1 3′-UTR or BRG1 3′-UTR with mutation at the predicted miR-21-5p target sequence were cotransfected into SW48 cells, along with miR-21-5p mimics (miR-21-5p); the negative control and relative luciferase activity was assayed. *, $P < 0.05$; ***, $P < 0.001$. **D,** Reporter constructs containing either wild-type BRG1 3′-UTR or BRG1 3′-UTR with mutation at the predicted miR-155-5p target sequence were cotransfected into SW48 cells, along with miR-155-5p mimics (miR-155-5p); the negative control and relative luciferase activity were assayed. ***, $P < 0.001$. **E,** Reporter constructs containing either wild-type BRG1 3′-UTR or BRG1 3′-UTR with mutation at the predicted miR-21-5p target sequence were cotransfected into SW48 cells, along with miR-21-5p inhibitor (Inh-21-5p); the negative control and relative luciferase activity was assayed. **, $P < 0.01$. **F,** Reporter constructs containing either wild-type BRG1 3′-UTR or BRG1 3′-UTR with mutation at the predicted miR-155-5p target sequence were cotransfected into SW48 cells, along with miR-155-5p inhibitor (Inh-155-5p); the negative control and relative luciferase activity was assayed (**, $P < 0.01$).

miR-130b-3p, and miR-378e. miR-21-5p, miR-340-5p, and miR-192-5p were found as the most miRNAs in M2-derived exosomes. We then used RT-PCR and confirmed their expression pattern in SW48 cells cocultured with M2-derived exosomes. The results showed that miR-21-5p and miR-155-5p had the largest fold difference in expression levels between SW48 and SW48 treated with M2-exo (Fig. 3A). To verify the expression of miR-21-5p and miR-155-5p in M2 macrophage–derived exosomes, we used the exosomes collected from CM of CAFs, HUVECs, and monocytes as controls. Results showed that M2 macrophage–derived exosomes revealed higher expression of miR-21-5p and miR-155-5p in M2 macrophage–derived exosomes than the controls (Supplementary Fig. S3C). We transfected M2 macrophages with Cy3-labeled miR-21-5p and miR-155-5p, then SW48 cells were cocultured with Cy3-miR-21-5p or Cy3-miR-155-5p–transfected macrophages using the 0.4-μm pore size Transwell. After 48 hours, $Cy3^+$ SW48 cells could be detected by immunofluorescence and flow cytometry, which further suggested the transfer of miR-21-5p and miR-155-5p from M2 macrophage to colon cancer cells (Fig. 3B; Supplementary Fig. S3D). We then transfected miR-21-5p or miR-155-5p inhibitors into the macrophages. The exosomes derived from these macrophages were collected and used in the function experiments *in vitro* and *in vivo*. Results showed that miR-21-5p or miR-155-5p inhibitors would decrease the expression of the corresponding miRNAs in exosomes (Supplementary Fig. S3E). The deletion of miR-21-5p and miR-155-5p disabled M2-derived exosomes to increase the motility of SW48 (Fig. 3C). M2-derived exosomes without miR-21-5p and miR-155-5p could no longer promote tumor cell migration and invasion *in vivo* (Fig. 3D and E). Collectively, exosomes derived from M2 macrophages primed colon cancer cells' motility by shuttling miR-21-5p and miR-155-5p into the colorectal cancer cells.

BRG1 is the target of miR-21-5p and miR-155-5p

miRNAs could bind with 3′ UTR of genes regulating the mRNA and protein expression (26). Public databases, miRTarBase (27) and miRWalk (28, 29), were used to predict their target genes. Data showed that there are 76 common target genes of miR-21-5p and miR-155-5p (Supplementary Fig. S4A–S4C). Then, David Bioinformatics Resources and literature review were used to analyze the functional annotation clustering of these 76 genes. Twelve genes were related to cancer cell metastasis (30). We used RT-PCR to detect the expression of these genes after treating with M2-derived exosomes. Results showed a significantly downregulated expression of BRG1 (Supplementary Fig. S4D). BRG1 was confirmed as the target gene of miR-21-5p and miR-155-5p. To evaluate the effect of miR-21-5p and miR-155-5p on BRG1 expression, we transfected miR-21-5p inhibitor and its mimics, and miR-155-5p inhibitor and its mimics. The results showed that miR-21-5p and miR-155-5p mimics could reduce BRG1 expression. In contract, their inhibitors could slightly increase BRG1 expression. Cotransfection of miR-21-5p mimics and miR-155-5p mimics revealed a stronger effect than just one used (Fig. 4A). To confirm whether BRG1 is a common direct target of miR-21-5p and miR-155-5p, wild-type or miRNA-binding site–mutant BRG1 3′-UTR–driven luciferase vector were cotransfected into SW48 cells with miR-21-5p or miR-155-5p mimics (Fig. 4B). Compared with control group, the overexpression of miR-21-5p or miR-155-5p inhibited luciferase activity of wild-type BRG1 3′-UTR. Furthermore, the inhibition was rescued by both miR-21-5p and miR-155-5p binding site mutation (Fig. 4C and D). Conversely, cotransfection of miR-21-5p inhibitor (Inh-miR-21-5p) or miR-155-5p inhibitor (Inh-miR-155-5p) notably increased the firefly luciferase activity of reporter with wild-type 3′-UTR of BRG1, but no that of the mutant reporter (Fig. 4E and F). Collectively, our finding indicated that BRG1 was the target of miR-21-5p and miR-155-5p.

MDE promoting colorectal cancer cells' migration and invasion depends on BRG1

We have previously found that decreased BRG1 expression participates in colorectal cancer metastasis via activating Wnt/β-catenin signaling pathway *in vitro* and *in vivo* (31). Depletion of BRG1 in SW48 cells would elevate cell migration and invasion. The phenotype was as strong as the M2-derived exosomes (Supplementary Fig. S5A and S5B). After SW48 cells were incubated with exosomes isolated from M2 macrophages, BRG1 protein levels were significantly reduced (Fig. 5A; Supplementary Fig. S6A). Downregulated BRG1 expression could be rescued by cotransfecting SW48 cells with miR-21-5p inhibitor and miR-155-5p inhibitor (Fig. 5B; Supplementary Fig. S6B). When the delivery of miR-21-5p and miR-155-5p was blocked by transfecting M2 with miR-21-5p inhibitor and miR-155-5p inhibitor, the M2 exosome was unable to suppress the expression of BRG1 (Supplementary Fig. S6C and S6D). We detected the expression level of BRG1 in the lungs of mice through IHC assays. We found that few BRG1 proteins were stained in lung metastasis of exosome-treated mice (Fig. 5C). M2-derived exosomes could also reduce the firefly luciferase activity of reporter with wild-type 3′-UTR of BRG1, but no of the reporter containing both the miR-21-5p and miR155-binding sequence mutant (Fig. 5D). To further confirm that downregulated BRG1 by exosomes contributed to increasing motility of colorectal cancer cells, we infected SW48 cells with adenoviral vector BRG1-GFP or adenoviral vector GFP. Transfection efficiency was evaluated by fluorescence microscope (Supplementary Fig. S6E). Overexpression of BRG1 could inhibit the increased motility of SW48-exposed exosomes (Fig. 5E). *In vivo*, the overexpression of BRG1 could prevent invasion and migration of SW48 cells, which were treated with M2-derived exosomes (Supplementary Fig. S6F–S6H). PTEN had been reported as the target of miR-21-5p, to further confirm MDE-promoting colorectal cancer cells' migration and invasion depends on BRG1, CO-115 cells were treated with MDE, a reported PTEN-mutant cell line (32). We also found that MDE could promote CO-115 cells' migration and invasion, whereas when we rescue BRG1 expression in the cells, it could also suppress the MDE-induced cell migration and invasion (Fig. 5F). In addition, miR-21-5p mimics promoted migration and invasion in CO-115 cells, whereas miR-21-5p inhibitor decreased motility of CO-115 cells (Supplementary Fig. S7A). In CO-115 cells, miR-21-5p mimics could reduce BRG1 expression and its inhibitors could increase BRG1 expression (Supplementary Fig. S7B). After CO-115 cells were incubated with exosomes isolated from M2 macrophages, BRG1 protein levels were also significantly reduced (Supplementary Fig. S7C). All these data indicated that BRG1 was the major factor for MDE-inducing cell migration and invasion.

TAMs are enriched and positively related with cancer metastasis in colorectal cancer

We analyzed public gene expression profiles to find out the relationship between BRG1 and the specific markers of some

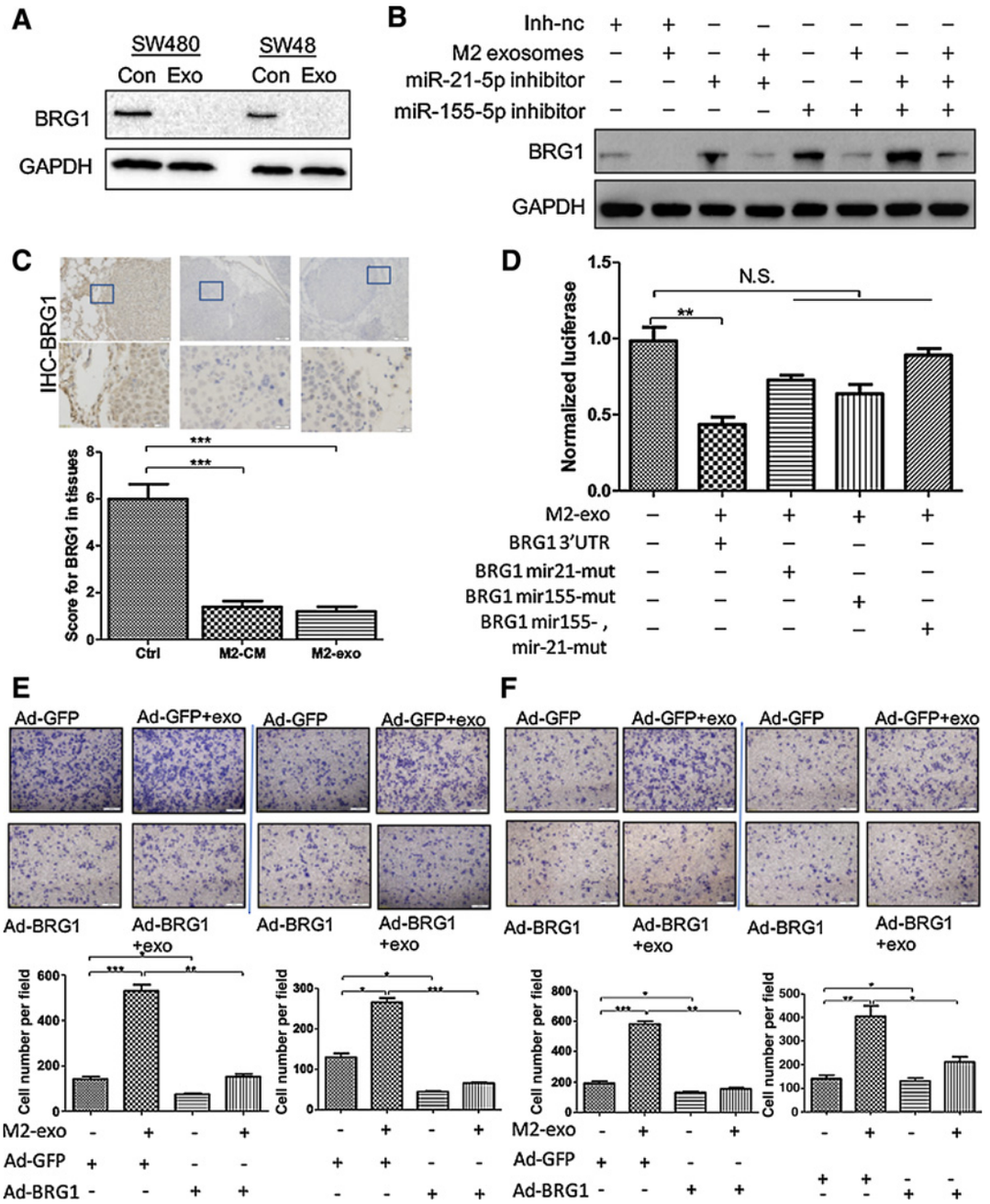

Figure 5.

MDE promoting colorectal cancer cell migration and invasion depends on BRG1. **A,** The protein expression analysis of BRG1 in SW480 and SW48 cells incubated with FBS-free media or M2-exo. **B,** The protein expression analysis of BRG1 in S48 transfected with inhibitor negative control, miR-21-5p inhibitor, or miR-155-5p inhibitor after incubation with or without M2-exosomes. **C,** BRG1 staining in SW48 cell lung metastatic site. First panel, scale bar, 200 μm; second panel, scale bar, 20 μm; third panel, the score of BRG1 expression in lung metastasis; ***, $P < 0.001$. **D,** Reporter constructs containing either wild-type BRG1 3′-UTR or BRG1 3′-UTR with mutation at the predicted miR-155-5p or/and miR-21-5p-5p target sequences were transfected into SW48 cells, along with M2-exo, and relative luciferase activity was assayed. **, $P < 0.01$. **E,** Cell migration assays using Transwell (left, representative pictures of Transwell chambers; right, average counts from three times of independent testing) in SW48 Ad-GFP or SW48 Ad-BRG1 incubated with or without M2-exo. **, $P < 0.01$; ***, $P < 0.0001$. **F,** Cell migration assays using Transwell (left, representative pictures of transwell chambers; right, average counts from three times of independent testing) in CO-115 Ad-GFP or CO-115 Ad-BRG1 incubated with or without M2-exo. **, $P < 0.01$; ***, $P < 0.0001$.

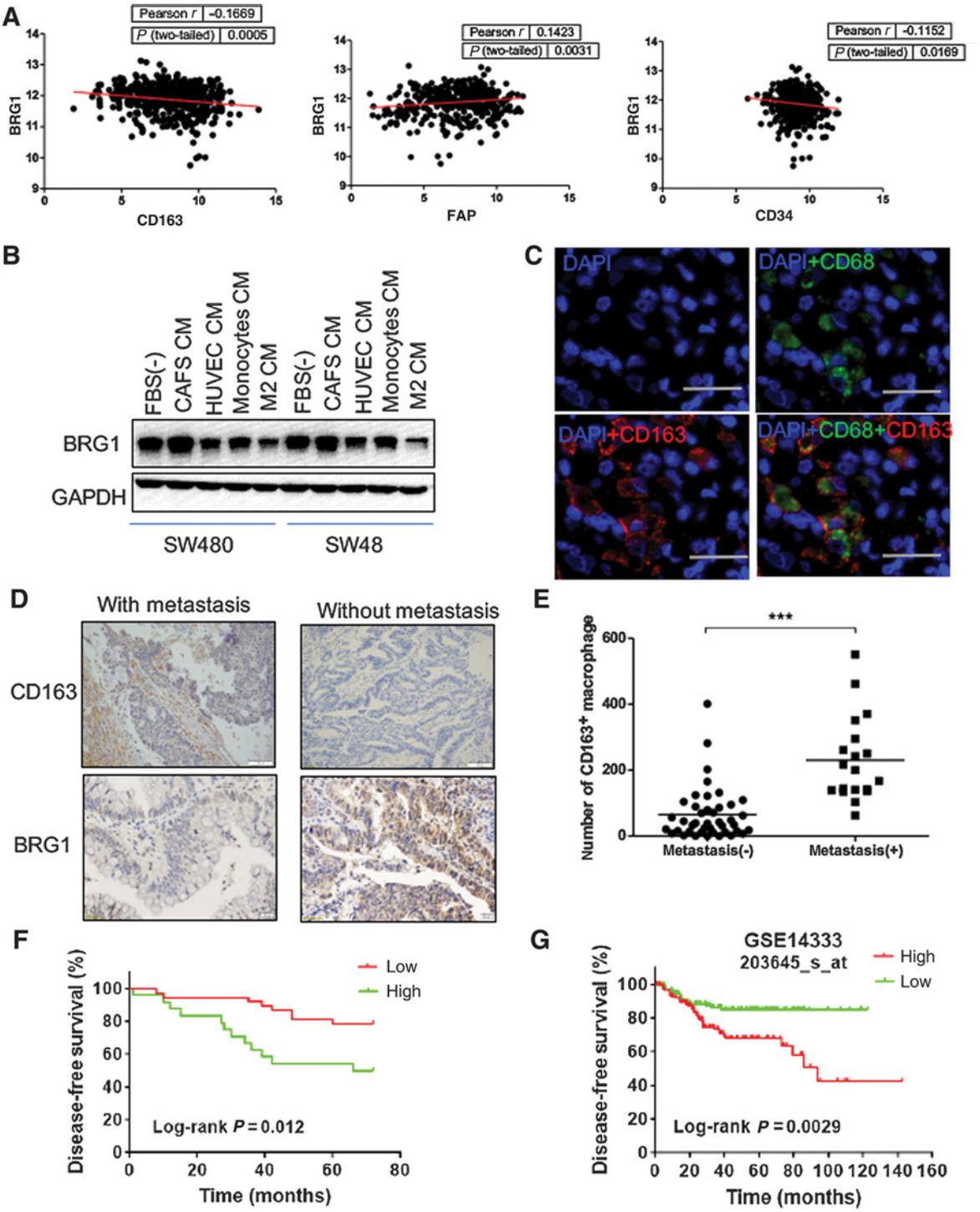

Figure 6.

TAMs regulate the expression level of BRG1 and are related to cancer metastasis in colon cancers**. A,** Pearson *r* correlation was used to analyze the relationship between BRG1 and CD163, FAP, or CD34. **B,** Western blot analysis of BRG1 protein expression in SW480 and SW48 cells after coculture with CM collected from CAFs, HUVECs, monocytes, and M2. **C,** Analysis of the phenotype of macrophages in colorectal cancer tissues by immunofluorescence. Scale bar, 50 μm. **D,** CD163 staining in colorectal cancer with metastasis or without metastasis. Scale bar, 100 μm. **E,** Positive cell number of CD163 staining in 42 primary colorectal cancers without metastasis or 19 colorectal cancers with metastasis. ***, $P < 0.001$. **F,** Kaplan–Meier analysis of overall survival for 61 diagnosed patients with colorectal cancer according to positive cell number of CD163 staining ($P = 0.012$). **G,** Survival analysis of 226 diagnosed patients with colorectal cancer–based CD163 mRNA levels in GEO cohorts (GSE14333).

Table 1. The relationship of expression of CD163 with metastasis (χ^2 test)

	CD163 Staining		
	Low (%)	High (%)	*P*
Gender			0.6012
Male	22	16	
Female	15	8	
T			0.0007
T1, T2	11	18	
T3, T4	26	6	
Differentiation			0.0309
Better	24	22	
Worse	13	2	
Lymph node metastasis			<0.0001
Negative	35	10	
Positive	2	14	
Distant metastasis			0.0099
Negative	35	16 (39.0)	
Positive	2	8	
Stage			<0.0001
I, II	34	6	
III, IV	3	18	

nontumorous cells in tumor microenvironment. The association between BRG1 and CD163, FAP or CD34 expression from TCGA was analyzed using the Pearson *r* correlation test. BRG1 and FAP, the marker of cancer-associated fibroblasts, had a significant positive correlation ($r = 0.1423$, $P = 0.0031$). A negative but less significant correlation between BRG1 and CD34, the marker of epithelial cells, was revealed ($r = -0.1152$, $P = 0.0169$), whereas we observed a significant negative correlation between BRG1 and CD163, a M2 macrophage marker, at mRNA levels ($r = -0.1669$, $P = 0.0005$; Fig. 6A). To further confirm this result, we treated SW48 and SW480 colon cancer cells with CM collected from CAFs, HUVECs, M2, and monocytes. We found that only CM from M2 macrophage could reduce BRG1 protein level significantly (Fig. 6B; Supplementary Fig. S8).

To further confirm the public database results, we measured TAM infiltration in 61 colorectal cancer clinical specimens. The distribution of $CD163^+$ macrophages in colorectal cancer tissues was found at the stromal of tumor and around the blood vessels (Fig. 6C and D). The number of TAMs varied from 0 to 688 per field. An average value was taken to separate samples into those with low (<116 per field) and high (≥116 per field) number of TAMs. Data showed that counts of $CD163^+$ macrophage was positively correlated with colorectal cancer metastasis and tumor stage (Fig. 6D; Table 1), whereas in metastasis-positive cases, the counts of $CD163^+$ M2 were higher than metastasis-negative cases (Fig. 6E). These indicated that M2 macrophages might contribute to colorectal cancer metastasis. We assessed the association of $CD163^+$ macrophage in colorectal cancer tumor tissue with clinical outcome and found that patients with much more $CD163^+$ macrophages had more reduced survival than patients with less $CD163^+$ macrophages (Fig. 6F). Reduced tumor CD163 mRNA levels were positively correlated with shortened patient survival when SurvExpress was employed (Fig. 6G).

Discussion

The communication between colon cancer cells and the tumor-educated macrophages reprograms macrophages to create a microenvironment for tumor growth; this microenvironment enables tumor cells to metastasize after accomplishing a series of biological steps (33). Recent studies have shown that the communication between cells could be mediated by exosomes (25), which could engulfed local tissues immediately or swarm into body fluid to affect distant target organs through endocytosis (34). In this study, we showed that CM collected from M2 macrophages could promote colorectal cancer cell motility, migration, and invasion with the help of M2 macrophage–derived exosomes. Previous studies have reported other molecules involved in the macrophage stimulation of migration, such as IL6, TNFα, Wnt5a, and EGF (11, 35–37).

miR-21-5p has been reported upregulated in several kinds of cancers, but why cancer cell expressed high level of miR-21-5p is still unclear (38). Noncoding RNAs are contained in exosomes, according to recent studies (39). miR-21-5p has been detected in exosome-derived ovarian cancer associate fibroblasts dendritic cells, breast cancer cells, T cells, and serum samples. Moreover, miR-155-5p was also found in exosomes of serum from patients with hematoma carcinoma (22). In this study, we identified that miR-21-5p and miR-155-5p were of high expression in MDE, and MDE shuttled miR-21-5p and miR-155-5p into colorectal cancer cells. miR-21-5p was a protumor miRNA, which targets to PTEN, P21, PDCD4, and APAF1, promoting cell growth and inducing chemotherapeutic resistance in breast and ovarian cancer (22, 40, 41). miR-155-5p was also regarded as an "OncomiR," which has been shown to target SOCS1, FOXO3, and cytokine signaling 1 gene for inducing breast cancer cell proliferation and chemosensitivity (42, 43). Here, we demonstrated that miR-21-5p and miR-155-5p can be transferred by exosomes from macrophages to tumor cells. This could probably happen in surrounding vessels and enable the tumor cells in the vessel–cancer interface to migrate more aggressively. This may facilitate the more invasive tumor cells to migrate into blood vessels.

The SWItch/Sucrose Non-Fermentable(SWI/SNF) complex was involved in regulation of gene transcription by remodeling chromatin in a ATP-dependent manner (44). It has been reported that it participates in early embryonic development, inflammation, and immune response (44–47). BRG1, a core motor of SWI/SNF, is decreased in cancer tissues identified by several studies (48, 49). It has been reported that BRG1 mutation or silence occurs in primary lung tumors and several cancers (50–52).In our previous paper, we show that loss of BRG1 induces colorectal cancer cell senescence through the p53/p21 pathway. We demonstrate that BRG1 binds to SIRT1 and interferes with SIRT1-mediated deacetylation of p53 at K382 (53). We also have a previous paper showing that the loss of BRG1 promotes colorectal cancer cell metastasis though Wnt pathway. Combining our results, we demonstrate the different roles of BRG1 in cell proliferation and metastasis (31), but it is still unknown why BRG1 is downregulated in colon cancers. In this study, we focus on the colorectal cancer cells' migration and invasion and investigate that MDE downregulate BRG1 through miR-21-5p and miR-155-5p and promote cell migration and invasion in colon cancer. Furthermore, there is also a published paper showing that high levels of oncomiR-21 contribute to the senescence-induced growth arrest in normal human cells (54), which supports our conclusion. However, in this study, we did not examine exosomes derived from the tumor cells to macrophages. Here we showed that macrophages could promote colorectal cancer metastasis, but the effect of colorectal cancer on macrophage was not examined. In the future, we would focus on the effect of colorectal cancer on macrophage. Colorectal cancer might educate macrophage into a supportive role.

Collectively, our finding shows that transfer of exosomes from M2 macrophages to colon cancer cells represents an undescribed mechanism that explains the manner in which immune cells are involved into tumor progression. Preventing this transfer is likely a new strategy for suppressing colon cancer metastasis.

Disclosure of Potential Conflicts of Interest

No potential conflicts of interest were disclosed.

Authors' Contributions

Conception and design: L. Sun, X. Yuan, G. Wang
Development of methodology: L. Sun, X. Yuan
Acquisition of data (provided animals, acquired and managed patients, provided facilities, etc.): J. Lan, L. Sun, F. Xu, L. Liu, F. Hu, D. Song, Z. Hou, W. Wu, X. Yuan
Analysis and interpretation of data (e.g., statistical analysis, biostatistics, computational analysis): L. Sun, X. Luo, J. Wang, X. Yuan, G. Wang
Writing, review, and/or revision of the manuscript: L. Sun, X. Yuan, J. Hu, G. Wang
Administrative, technical, or material support (i.e., reporting or organizing data, constructing databases): L. Sun, X. Yuan, G. Wang
Study supervision: L. Sun, X. Luo, X. Yuan, J. Hu

Acknowledgments

We are grateful to the members in G. Wang's lab and J. Hu's lab for the critical inputs and suggestions. This work is supported by NSFC grants (no. 81572725 to J. Hu; nos. 81570525 and 81773113 to G. Wang), `973' program (no. 2015CB553903-1 to J. Hu) and grant from the Huazhong University of Science and Technology "Double Top" Construction Project of International Cooperation (grant no. 540-5001540013 to X.L. Yuan).

The costs of publication of this article were defrayed in part by the payment of page charges. This article must therefore be hereby marked *advertisement* in accordance with 18 U.S.C. Section 1734 solely to indicate this fact.

Received January 3, 2018; revised July 3, 2018; accepted November 2, 2018; published first November 6, 2018.

Reference

1. Joyce JA, Pollard JW. Microenvironmental regulation of metastasis. Nat Rev Cancer 2009;9:239–52.
2. Pollard JW. Trophic macrophages in development and disease. Nat Rev Immunol 2009;9:259–70.
3. Pollard JW. Tumour-educated macrophages promote tumour progression and metastasis. Nat Rev Cancer 2004;4:71–8.
4. Ojalvo LS, King W, Cox D, Pollard JW. High-density gene expression analysis of tumor-associated macrophages from mouse mammary tumors. Am J Pathol 2009;174:1048–64.
5. Qian BZ, Pollard JW. Macrophage diversity enhances tumor progression and metastasis. Cell 2010;141:39–51.
6. Caronni N, Savino B, Bonecchi R. Myeloid cells in cancer-related inflammation. Immunobiology 2015;220:249–53.
7. Sica A, Erreni M, Allavena P, Porta C. Macrophage polarization in pathology. Cell Mol Life Sci 2015;72:4111–26.
8. Wyckoff JB, Wang Y, Lin EY, Li JF, Goswami S, Stanley ER, et al. Direct visualization of macrophage-assisted tumor cell intravasation in mammary tumors. Cancer Res 2007;67:2649–56.
9. Hagemann T, Robinson SC, Schulz M, Trumper L, Balkwill FR, Binder C. Enhanced invasiveness of breast cancer cell lines upon co-cultivation with macrophages is due to TNF-alpha dependent up-regulation of matrix metalloproteases. Carcinogenesis 2004;25:1543–9.
10. Vasiljeva O, Papazoglou A, Kruger A, Brodoefel H, Korovin M, Deussing J, et al. Tumor cell-derived and macrophage-derived cathepsin B promotes progression and lung metastasis of mammary cancer. Cancer Res 2006;66:5242–50.
11. Pukrop T, Klemm F, Hagemann T, Gradl D, Schulz M, Siemes S, et al. Wnt 5a signaling is critical for macrophage-induced invasion of breast cancer cell lines. Proc Natl Acad Sci U S A 2006;103:5454–9.
12. Pan BT, Johnstone RM. Fate of the transferrin receptor during maturation of sheep reticulocytes *in vitro*: selective externalization of the receptor. Cell 1983;33:967–78.
13. Raposo G, Nijman HW, Stoorvogel W, Liejendekker R, Harding CV, Melief CJ, et al. B lymphocytes secrete antigen-presenting vesicles. J Exp Med 1996;183:1161–72.
14. Raposo G, Tenza D, Mecheri S, Peronet R, Bonnerot C, Desaymard C. Accumulation of major histocompatibility complex class II molecules in mast cell secretory granules and their release upon degranulation. Mol Biol Cell 1997;8:2631–45.
15. Thery C, Regnault A, Garin J, Wolfers J, Zitvogel L, Ricciardi-Castagnoli P, et al. Molecular characterization of dendritic cell-derived exosomes. Selective accumulation of the heat shock protein hsc73. J Cell Biol 1999;147:599–610.
16. van Niel G, Porto-Carreiro I, Simoes S, Raposo G. Exosomes: a common pathway for a specialized function. J Biochem 2006;140:13–21.
17. Blanchard N, Lankar D, Faure F, Regnault A, Dumont C, Raposo G, et al. TCR activation of human T cells induces the production of exosomes bearing the TCR/CD3/zeta complex. J Immunol 2002;168:3235–41.
18. Peinado H, Aleckovic M, Lavotshkin S, Matei I, Costa-Silva B, Moreno-Bueno G, et al. Melanoma exosomes educate bone marrow progenitor cells toward a pro-metastatic phenotype through MET. Nat Med 2012;18:883–91.
19. Taylor DD, Gercel-Taylor C. Exosomes/microvesicles: mediators of cancer-associated immunosuppressive microenvironments. Semin Immunopathol 2011;33:441–54.
20. Luga V, Zhang L, Viloria-Petit AM, Ogunjimi AA, Inanlou MR, Chiu E, et al. Exosomes mediate stromal mobilization of autocrine Wnt-PCP signaling in breast cancer cell migration. Cell 2012;151:1542–56.
21. Cassetta L, Noy R, Swierczak A, Sugano G, Smith H, Wiechmann L, et al. Isolation of mouse and human tumor-associated macrophages. Adv Exp Med Biol 2016;899:211–29.
22. Au Yeung CL, Co NN, Tsuruga T, Yeung TL, Kwan SY, Leung CS, et al. Exosomal transfer of stroma-derived miR21 confers paclitaxel resistance in ovarian cancer cells through targeting APAF1. Nat Commun 2016;7:11150.
23. Zhou W, Fong MY, Min Y, Somlo G, Liu L, Palomares MR, et al. Cancer-secreted miR-105 destroys vascular endothelial barriers to promote metastasis. Cancer Cell 2014;25:501–15.
24. Muller G. Microvesicles/exosomes as potential novel biomarkers of metabolic diseases. Diabetes Metab Syndr Obes 2012;5:247–82.
25. Cocucci E, Racchetti G, Meldolesi J. Shedding microvesicles: artefacts no more. Trends Cell Biol 2009;19:43–51.
26. Bartel DP. MicroRNAs: genomics, biogenesis, mechanism, and function. Cell 2004;116:281–97.
27. Chou CH, Shrestha S, Yang CD, Chang NW, Lin YL, Liao KW, et al. miRTarBase update 2018: a resource for experimentally validated microRNA-target interactions. Nucleic Acids Res 2018;46:D296–302.
28. Dweep H, Gretz N. miRWalk2.0: a comprehensive atlas of microRNA-target interactions. Nat Methods 2015;12:697.
29. Dweep H, Sticht C, Pandey P, Gretz N. miRWalk–database: prediction of possible miRNA binding sites by "walking" the genes of three genomes. J Biomed Inform 2011;44:839–47.
30. Huang da W, Sherman BT, Lempicki RA. Systematic and integrative analysis of large gene lists using DAVID bioinformatics resources. Nat Protoc 2009;4:44–57.
31. Wang G, Fu Y, Yang X, Luo X, Wang J, Gong J, et al. Brg-1 targeting of novel miR550a-5p/RNF43/Wnt signaling axis regulates colorectal cancer metastasis. Oncogene 2016;35:651–61.
32. Ahmed D, Eide PW, Eilertsen IA, Danielsen SA, Eknaes M, Hektoen M, et al. Epigenetic and genetic features of 24 colon cancer cell lines. Oncogenesis 2013;2:e71.

33. Szebeni GJ, Vizler C, Kitajka K, Puskas LG. Inflammation and cancer: extra- and intracellular determinants of tumor-associated macrophages as tumor promoters. Mediators Inflamm 2017;2017:9294018.
34. Simons M, Raposo G. Exosomes–vesicular carriers for intercellular communication. Curr Opin Cell Biol 2009;21:575–81.
35. Naugler WE, Sakurai T, Kim S, Maeda S, Kim K, Elsharkawy AM, et al. Gender disparity in liver cancer due to sex differences in MyD88-dependent IL-6 production. Science 2007;317:121–4.
36. Hagemann T, Wilson J, Kulbe H, Li NF, Leinster DA, Charles K, et al. Macrophages induce invasiveness of epithelial cancer cells via NF-kappaB and JNK. J Immunol 2005;175:1197–205.
37. Wyckoff J, Wang W, Lin EY, Wang Y, Pixley F, Stanley ER, et al. A paracrine loop between tumor cells and macrophages is required for tumor cell migration in mammary tumors. Cancer Res 2004;64:7022–9.
38. Ferraro A, Kontos CK, Boni T, Bantounas I, Siakouli D, Kosmidou V, et al. Epigenetic regulation of miR-21 in colorectal cancer: ITGB4 as a novel miR-21 target and a three-gene network (miR-21-ITGBeta4-PDCD4) as predictor of metastatic tumor potential. Epigenetics 2014;9:129–41.
39. Valadi H, Ekstrom K, Bossios A, Sjostrand M, Lee JJ, Lotvall JO. Exosome-mediated transfer of mRNAs and microRNAs is a novel mechanism of genetic exchange between cells. Nat Cell Biol 2007;9:654–9.
40. Meng F, Henson R, Wehbe-Janek H, Ghoshal K, Jacob ST, Patel T. MicroRNA-21 regulates expression of the PTEN tumor suppressor gene in human hepatocellular cancer. Gastroenterology 2007;133: 647–58.
41. Si ML, Zhu S, Wu H, Lu Z, Wu F, Mo YY. miR-21-mediated tumor growth. Oncogene 2007;26:2799–803.
42. Lei K, Du W, Lin S, Yang L, Xu Y, Gao Y, et al. 3B, a novel photosensitizer, inhibits glycolysis and inflammation via miR-155–5p and breaks the JAK/STAT3/SOCS1 feedback loop in human breast cancer cells. Biomed Pharmacother 2016;82:141–50.
43. Kong W, He L, Coppola M, Guo J, Esposito NN, Coppola D, et al. *MicroRNA*-155 regulates cell survival, growth, and chemosensitivity by targeting FOXO3a in breast cancer. J Biol Chem 2010;285: 17869–79.
44. Whitehouse I, Flaus A, Cairns BR, White MF, Workman JL, Owen-Hughes T. Nucleosome mobilization catalysed by the yeast SWI/SNF complex. Nature 1999;400:784–7.
45. Wilson BG, Roberts CW. SWI/SNF nucleosome remodellers and cancer. Nat Rev Cancer 2011;11:481–92.
46. Ramirez-Carrozzi VR, Nazarian AA, Li CC, Gore SL, Sridharan R, Imbalzano AN, et al. Selective and antagonistic functions of SWI/SNF and Mi-2beta nucleosome remodeling complexes during an inflammatory response. Genes Dev 2006;20:282–96.
47. Han D, Jeon S, Sohn DH, Lee C, Ahn S, Kim WK, et al. SRG3, a core component of mouse SWI/SNF complex, is essential for extra-embryonic vascular development. Dev Biol 2008;315:136–46.
48. Reisman D, Glaros S, Thompson EA. The SWI/SNF complex and cancer. Oncogene 2009;28:1653–68.
49. Klochendler-Yeivin A, Muchardt C, Yaniv M. SWI/SNF chromatin remodeling and cancer. Curr Opin Genet Dev 2002;12:73–9.
50. Wong AK, Shanahan F, Chen Y, Lian L, Ha P, Hendricks K, et al. BRG1, a component of the SWI-SNF complex, is mutated in multiple human tumor cell lines. Cancer Res 2000;60:6171–7.
51. Valdman A, Nordenskjold A, Fang X, Naito A, Al-Shukri S, Larsson C, et al. Mutation analysis of the BRG1 gene in prostate cancer clinical samples. Int J Oncol 2003;22:1003–7.
52. Medina PP, Romero OA, Kohno T, Montuenga LM, Pio R, Yokota J, et al. Frequent BRG1/SMARCA4-inactivating mutations in human lung cancer cell lines. Hum Mutat 2008;29:617–22.
53. Wang G, Fu Y, Hu F, Lan J, Xu F, Yang X, et al. Loss of BRG1 induces colorectal cancer cell senescence by regulating p53/p21 pathway. Cell Death Dis 2017;8:e2607.
54. Dellago H, Preschitz-Kammerhofer B, Terlecki-Zaniewicz L, Schreiner C, Fortschegger K, Chang MW, et al. High levels of oncomiR-21 contribute to the senescence-induced growth arrest in normal human cells and its knock-down increases the replicative lifespan. Aging Cell 2013;12:446–58.